International Journal of Mechanical Sciences 142–143 (2018) 480–490

Contents lists available at ScienceDirect

International Journal of Mechanical Sciences

journal homepage: www.elsevier.com/locate/ijmecsci

Comparison of flow structures behind rigid and flexible finite cylinders

Sung Yong Jung [a], Jeong Jae Kim [b], Han Wook Park [b], Sang Joon Lee [b,c,*]

[a] Department of Mechanical Engineering, Chosun University, 309 Pilmun-Daero, Dong-gu, Gwangju 61452, South Korea
[b] Department of Mechanical Engineering, Pohang University of Science and Technology (POSTECH), 77 Cheongam-Ro. Nam-Gu. Pohang. Gyeongbuk, Korea 37673, South Korea
[c] Center for Biofluid and Biomimic Research, POSTECH, 77 Cheongam-Ro. Nam-Gu. Pohang. Gyeongbuk. Korea 37673, South Korea

ARTICLE INFO

Keywords:
Flexible cylinder
Wake structure
Particle image velocimetry
Proper orthogonal decomposition

ABSTRACT

Flows over bluff bodies are closely related to aero- or hydro-dynamic forces on structures. In bio-mimetic applications, flexible structures are usually employed, and quantitative flow information is essential for optimizing structural design. In this study, the flow behind a flexible cylinder is compared with the flow behind a rigid cylinder using flow visualization, time-resolved particle image velocimetry (PIV), and proper orthogonal decomposition (POD) modal analysis. The spectral analysis demonstrates that the oscillatory motion of a flexible cylinder strongly influences the flow behind the cylinder. The flows behind the rigid and flexible cylinders are clearly different near the free end of the cylinder. The downwash flow from the free end of the flexible cylinder is relatively weak compared to the rigid cylinder. Behind the tip of the flexible cylinder, large-scale vortices are shed and they are propagated downstream. However, such flow phenomena are not observed behind the rigid cylinder. These results could be used as basic data in the design process of bio-inspired structural applications.

1. Introduction

The flow around bluff bodies is a typical problem, not only in engineering fields, but also in nature and bio-inspired applications. Compared to typical engineering structures, the most distinctive characteristics of structures in nature are flexibility and deformability by fluid loading. In spite of these differences, aerodynamic or hydrodynamic forces on structures are the most common interest. These forces are closely related to flow structures around bodies, especially vortex generation and its downstream transport. Therefore, the flow behind a circular cylinder has been widely studied owing to its simple geometry and relevance to practical applications. However, in spite of its geometrical simplicity of cylinders, the flow behind a cylinder has complicated three-dimensional flow structures. The flow dynamics are strongly dependent on Reynolds numbers, and the three-dimensionality is enhanced with increasing Reynolds number [1–3].

The flow structure behind a circular cylinder is also closely related to the movement and mechanical properties of the cylinder [4–7]. In particular, the effect of the oscillating motion of a circular cylinder on the flow structure in near wake has been investigated [4,6]. The oscillating body has a significant influence on shear-layer instability and vortex formation, and the flow structure varies with the change in oscillating frequency. Williamson and Govardhan [7] reviewed the vortex dynamics and structural vibration of an elastically mounted cylinder reporting that a body motion induces change wake patterns. Huera-Huarte and Bearman [5] measured the drag coefficients and vortex structures of a long flexible cylinder. They observed different modes of vortex shedding, depending on the position and response of the cylinder.

The flow structures around a finite cylinder are different from those behind a 2D cylinder, which has been the primary focus of the study. The three-dimensionality of the wake becomes strong owing to downwash flows behind the free end of the finite cylinder. The flow structure depends on many factors, including upstream flow uniformity, aspect ratio, and shape of the cylinder [8–12]. The 3D topology and temporal dynamic behavior of the flow above the finite end was experimentally examined by Hain, Kähler and Michaelis [8]. In a different study, Park and Lee [10] reported that the vortex shedding frequency decreases and the vortex formation region elongates, as the aspect ratio decreases. Park and Lee [11] investigated the effect of upstream flow on vortex formation. The vortex shedding frequency and the length of the vortex formation region were diminished in boundary layers, compared to those under uniform flow condition. Park and Lee [9] observed the flow structures around the free end with different corner shapes. Sumner [12] reviewed the effect of various factors on the wake and vortex patterns of a finite circular cylinder. According to many previous studies, flow structures significantly change based on the critical aspect ratio, although the critical values vary depending on experimental conditions.

Although many studies have been conducted on the flow around finite cylinders, the cylinders tested in these studies were rigid. In nature and bio-inspired applications, cylindrical structures are flexible and have finite heights [13,14]. Recent studies have focused on flexi-

* Corresponding author.
E-mail address: sjlee@postech.ac.kr (S.J. Lee).

https://doi.org/10.1016/j.ijmecsci.2018.05.026
Received 3 July 2017; Received in revised form 17 January 2018; Accepted 9 May 2018

Table 1
Comparison of specifications between flexible and rigid cylinders used in the present study.

Specifications	FC	RC
Length (L)	70 mm	
Diameter (D)	3 mm	
Aspect ratio (AR = L/D)	23.3	
Freestream velocity (U_0)	3.5 m/s	
Reynolds number (Re)	673	
Mass ratio (ρ_c/ρ_f)	774.8	629.1
Young's modulus (E)	1.78 Mpa	530.85 Mpa
Bending rigidity (EI)	7.06 Nmm^2	2110.69 Nmm^2
Rotation stiffness (κ)	0.41 Nmm	90.46 Nmm
Natural frequency (f_n)	3.78 Hz	83.3 Hz

ble structures from the perspective of drag reduction through their reconfiguration [15–17]. The flows around these structures have also been investigated [14,18–21]. As aforementioned, quantitative flow information is essential to understand the dynamic forces exerted on flexible structures. However, most previous studies have focused on qualitative flow information around a flexible cylindrical structure [14] or quantitative flow information behind flexible flat plates [19–21], which are quite different from those of circular cylinders.

The main objective of this study is to compare the flow structures behind finite rigid and flexible cylinders. Flow field analysis is carried out using a time-resolved particle image velocimetry (PIV) technique and the flow visualization method. To investigate the differences in dominant turbulent structures, the proper orthogonal decomposition (POD) modal analysis is also employed in this study.

2. Experimental apparatus and methods

The experiments were carried out in a closed-type subsonic wind tunnel with a test section of 0.15 m (width) × 0.15 m (height) × 1.8 m (length). A model of a flexible cylinder (FC) having length L = 70 mm, diameter D = 3 mm was made of polydimethylsiloxane (PDMS), and a corresponding aspect ratio of L/D = 23.3. PDMS was synthesized with Sylgard 184 silicone elastomer base and Sylgard 184 silicone elastomer curing agent. The mechanical properties of a PDMS cylinder vary with the base/agent ratio and aspect ratio of the cylinder. In this study, the mechanical properties were measured through a bending test with pinpoint loading. The Young's modulus E and the rotation stiffness κ were estimated using a simple beam theory. The measured E, κ and bending rigidity EI were 1.78 MPa, 0.41 Nmm and 7.06 Nmm^2, respectively. The density of FC was 0.95 g/cm^3, and the mass ratio (ρ_c/ρ_f), which is ratio of material density to fluid density, was 774.8. The natural frequency of FC was 3.78 Hz.

A rigid cylinder (RC) model having the same physical dimensions as the FC model was made of poly lactic acid (PLA) using a 3D printer (MAKERBOT 4th replicator). The measured E, κ and EI were 530.85 MPa, 90.46 Nmm and 2110.69 Nmm^2, respectively. The density of RC was 0.77 g/cm^3, and ρ_c/ρ_f was 629.1. The natural frequency of RC was 83.3 Hz. The features of tested cylinder models are summarized in Table 1. The cylinder models were mounted on a PLA holder with holes at the center of the test section bottom. The blockage effect can be negligible because the blockage ratio of the test models was 0.93% in present study. The FC model had two degrees of freedom (DOF). The freestream velocity in the test section was fixed at $U_0 = 3.5$ m/s. The corresponding Reynolds number (*Re*) was 673, based on the cylinder diameter.

Fig. 1 shows a schematic of the experimental setup for simultaneous measurements of the cylinder motion and velocity fields of flows around the cylinder model. The origin of the coordinate system is the center of the free end surface of the cylinder. A high-speed camera (SA 1.1, Photron, USA) that can capture images of 1024 × 1024 pixels at 5400 frames per second (fps) and a maximum frame rate of 675,000 fps was employed in this study. The camera was installed in front of and above the wind tunnel to capture images in the x-z (side-view) and x-y plane (top-view), respectively. For gaseous flows, oil droplets are commonly used as seeding particles, because they have adequate aerodynamic response to velocity variations in wind tunnel studies [22,23]. Thus, olive oil particles with a mean diameter of approximately 1–3 μm were seeded as tracer particles. The corresponding Stokes number is 0.003–0.031. Since the Stokes number is much less than 0.1, the tracing error is smaller than 1% [24]. A thin laser light sheet was formed using an 8-W diode-pumped solid-state (DPSS) continuous laser (Changchun New Industries Optoelectronics Technology Co., China) with a wavelength of 532 nm. Flow images were consecutively recorded at a frame rate of 12,000 fps with 768 × 640 pixels. The pixel size with lens and the corresponding field of view were 0.0429 mm and 32.914 mm × 27.428 mm, respectively. The captured images were processed with an open-source tool for performing PIV analysis in Matlab [25,26]. A multigrid interrogation window scheme was adopted to extract instantaneous velocity fields with interrogation window sizes of 64 × 64, 32 × 32, and 16 × 16 pixels with 50% overlapping. In order to evaluate measurement

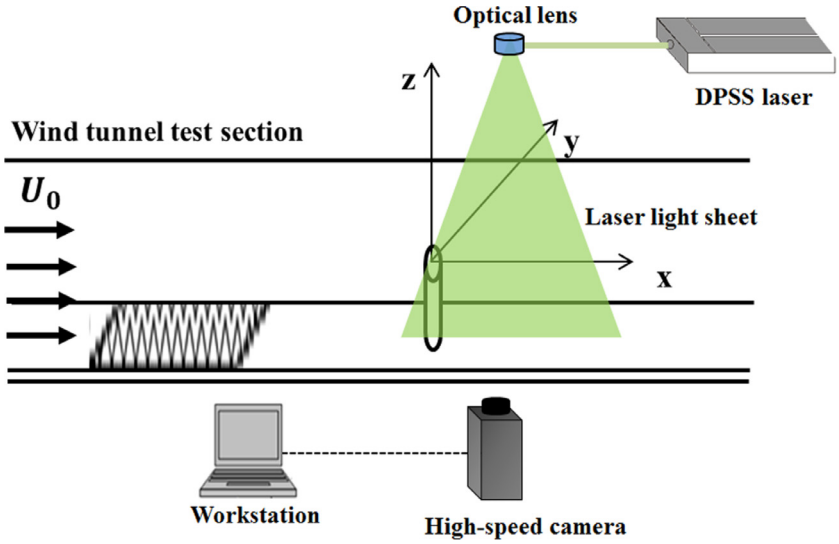

Fig. 1. A schematic diagram of the experimental setup with coordinate system for side view imaging. For top view (x-y plane) imaging, the position of a high-speed camera is switched with that of light sheet illumination.